

*Citation for published version:*

Pegg, EC, Walker, GS, Scotchford, CA, Farrar, D & Grant, D 2009, 'Mono-functional aminosilanes as primers for peptide functionalization', *Journal of Biomedical Materials Research - Part A*, vol. 90, no. 4, pp. 947-58.  
<https://doi.org/10.1002/jbm.a.32155>

*DOI:*

[10.1002/jbm.a.32155](https://doi.org/10.1002/jbm.a.32155)

*Publication date:*

2009

*Document Version*

Early version, also known as pre-print

[Link to publication](#)

## University of Bath

### Alternative formats

If you require this document in an alternative format, please contact:  
[openaccess@bath.ac.uk](mailto:openaccess@bath.ac.uk)

#### General rights

Copyright and moral rights for the publications made accessible in the public portal are retained by the authors and/or other copyright owners and it is a condition of accessing publications that users recognise and abide by the legal requirements associated with these rights.

#### Take down policy

If you believe that this document breaches copyright please contact us providing details, and we will remove access to the work immediately and investigate your claim.

# Monofunctional Aminosilanes as Primers for Peptide Functionalisation

Elise Pegg<sup>1</sup>, Gavin Walker<sup>1</sup>, Colin Scotchford<sup>1</sup>, David Farrar<sup>2</sup>, David Grant<sup>1</sup>

*1 Bioengineering Group, School of Mechanical Materials and Manufacturing Engineering, Department of Engineering, University of Nottingham, University Park, Nottingham, UK*

*2 Smith & Nephew Group Research Centre, York Science Park, Heslington, York, UK*

## Abstract

When covalently attaching biomolecules to surfaces such as titanium, trifunctional silanes are commonly used as primers to produce surface amine groups. However, these primed surfaces are rarely uniform in structure due to networking of the silane. Monofunctional aminosilanes may result in more uniform structures, although their long term stability and effect on osteoblast cell responses are possible issues for orthopaedic applications. This study examines for the first time the optimisation of peptide coupling to titanium using monofunctional aminosilane reaction chemistry. The resultant surface topography, chemistry and thicknesses were characterised showing improved surface uniformity compared to trifunctional silanised surfaces. The stability of the coatings was examined over a period of eight days in environments of varying pH, temperature and humidity. In addition, human osteosarcoma (HOS) cell adhesion and spreading on the samples was examined; adhesion was minimal on silanised surfaces, but after functionalisation with cysteine the cell density was greater than the titanium control and showed no overall detrimental effect on initial cell responses.

## Keywords

Surface modification; Titanium; Silane; Functionalisation; Degradation

## 1 Introduction

The idea of covalently attaching a biomolecule to the surface of an orthopaedic implant with the aim of triggering a specific cell response has great potential. It is fundamental that the method used to attach a biomolecule to the implant surface is; (a) stable enough to keep the biomolecule in place until the desired response is triggered, (b) that the active groups of the biomolecule are projected towards the cell and (c) that the components used to attach the biomolecule are not detrimental to cell function.

A method commonly employed to covalently attach biomolecules onto hydroxylated surfaces is functionalisation using an aminosilane reaction and subsequent chemical attachment using crosslinkers; this procedure has been successfully applied to biomaterials applications [1, 2, 3]. Trifunctional silanes are more commonly used because they react easily, are stable and are readily available. However, trifunctional silanes tend to polymerise and form networks on the surface, and even when experiments are performed in anhydrous environments the resultant surfaces are not uniform in structure [4, 5]. As a result of this, it is hard to model the reactions and draw conclusions from the structures produced.

Jonsson et al. [6] and subsequently Tripp et al. [7] have investigated gas phase reactions of mono-functional silanes and illustrated that reliable monolayers can be produced using this technique, although the equipment required for reactions in the vapour phase is expensive and has hazards associated with it. Monofunctional aminosilane coatings have been produced in anhydrous solvents [8, 5], although these surfaces are rarely functionalised with biomolecules and if they are, they are not fully characterised or optimised [9].

The question of whether monofunctional silanes are more [10, 11] or less stable [5] than trifunctional silanes has not been answered, as the conclusions in the literature conflict. The stability of silanised surfaces depends primarily upon the ease at which the siloxane bond with the substrate is hydrolysed. This in turn is dependent on the silane used, steric hindrance [12], hydrophobic interactions, degree of crosslinking and environmental conditions such as humidity [11, 13]; and differences in the methodology of the above studies could explain the discrepancies.

When considering the use of monofunctional silanes for orthopaedic applications there are two major concerns; stability (as discussed above) and toxicity. If the silane is cytotoxic but completely stable there is no issue provided that access to the silane is blocked by the crosslinked biomolecule. If the silane is not toxic but degrades easily then the bioactivity of the attached molecule might be compromised. However, if the silane degrades easily and is toxic then this would result in inflammation of the surrounding tissue which would be dependent on the quantity of attached silane released and the rate of degradation. This study aims to investigate these issues and examine the feasibility of monofunctional silanes as primers for functionalisation of titanium.

In the work presented here the reaction of monofunctional aminosilanes to titanium was characterised and optimised, and the subsequent functionalisation of cysteine to these surfaces examined. Samples produced through a three stage process (reaction scheme shown in figure 1) were then tested for stability in environments of varying pH, humidity and temperature. Finally, initial cell attachment responses to the samples at each reaction stage was performed to allow investigation of the cell responses to the changes in surface chemistry after each reaction, and give preliminary indication of any detrimental cell responses to the reagents.

## **2 Materials and Methods**

### **2.1 Sample Preparation**

Commercially pure grade 1 titanium sheet, 1 mm thick, was punched into 10 mm diameter discs, then polished to a mirror finish using 200, 400, 800, 1200  $\mu\text{m}$  grit paper then colloidal silica. Samples were then cleaned in acetone (> 97%, Sigma), ethanol (> 95%, Sigma) and triply distilled water (TDW) for 15 minutes using an ultrasonic bath. Before functionalisation samples were then further cleaned by ultrasonication in pure hydrochloric acid for 3 minutes and washed 5 times in distilled water.

### **2.2 Sample Oxidation**

To oxidise the titanium discs to increase hydroxyl groups, samples were ultrasonicated in piranha solution (concentrate sulphuric acid and 30 % hydrogen peroxide) 10 % v/v in water. These were then washed 3 times in distilled water.

### **2.3 Functionalisation of Titanium**

Samples were functionalised in three stages; firstly samples were silanised by immersing in a monofunctional aminosilane (3-aminopropyldimethylethoxysilane, APDMES, from Fluorochem, 4 % v/v in toluene) for 1 hour, washed 5 times in toluene (Stage 1). Samples were then immersed in 4-(N-maleimidomethyl)cyclohexane-1-carboxylic acid-3-sulfo-N-hydroxysuccinimide ester sodium salt (sulfo-SMCC, Sigma, 1.5 mg ml<sup>-1</sup> in phosphate buffered saline (PBS) solution for one hour, then washed 3 times with PBS and then TDW (Stage 2). The peptide (L-cysteine, Sigma, 2 mg ml<sup>-1</sup> in PBS) was then dissolved in degassed PBS in a nitrogen atmosphere and

reacted with all surfaces for 30 minutes (Stage 3). As a comparison a trifunctional silane, 3-aminopropyltriethoxy silane (APTES, Fluorochem), was also used instead of APDMES and it was reacted under the same conditions.

## **2.4 *Optimisation of Reaction Conditions***

Prior to full characterisation, the reaction conditions were optimised using infrared spectroscopy to monitor the reaction. The infrared spectrometer used to monitor the reactions was a Tensor 27 manufactured by Bruker, with an MCT nitrogen cooled detector and a resolution of  $2\text{ cm}^{-1}$ . Infrared Reflection Absorption Spectroscopy (IRRAS) was performed on the treated titanium discs using a horizontal reflection unit (grazing angle of  $80^\circ$ ) with a KR5 holographic polariser to maximise signal. The atmosphere inside the chamber was dried using purified air throughout and 30 s scans were taken for each spectrum.

The effect of: sample oxidation (with or without the oxidation process described in section 2.2); atmospheric humidity (reaction performed in a dry nitrogen atmosphere  $<100\text{ ppm}$  water, or air); silanisation time and silane concentration on the reaction was investigated. The reaction time was kept at 1 hour when varying silane concentrations and the silane concentration at 4 % v/v when examining reaction time. After the silanisation conditions were optimised, the concentration of sulfo-SMCC and cysteine was then varied and the optimum concentrations found using IRRAS.

## **2.5 *Characterisation of Functionalised Surfaces***

XPS analysis was performed using a Kratos AXIS ULTRA with mono-chromated Al K X-ray source (1486.6 eV). A pass energy of 20 eV was used for high resolution scans and 80 eV was used for wide scans. A charge correction was performed using the carbon 1s peak at 285 eV. The sample topography was examined using a Topometrix Explorer Pulsed-Force AFM in non-contact mode, with a resolution of 500 lines per scan and an area of  $125\text{ }\mu\text{m}^2$ . Data analysis involved 1<sup>st</sup> order levelling and the software used was WSxM (Nanotec Electronica, Spain). The coupling reaction was also analysed using dual polarisation interferometry (DPI) to determine the thickness of the coatings. An amine-functionalised chip (FB80 serial#0845) was used in an AnaLight® Bio200 DPI (Farfield Scientific Ltd) to represent the silanised surface. Fifty microlitres of the crosslinker (sulfo-SMCC,  $1.5\text{ mg ml}^{-1}$  in degassed PBS, Sigma) was flowed over the chip at a rate of  $30\text{ }\mu\text{l min}^{-1}$ ,

then washed with degassed PBS, followed by flowing 50  $\mu\text{l}$  of L-cysteine (2  $\text{mg ml}^{-1}$ , Sigma). The chip was then washed again with degassed PBS.

## **2.6 Stability tests**

Functionalised titanium samples were immersed in different environments for 8 days and were analysed every 24 hours using IRRAS and the immersion solutions replaced. The environments used were; triply distilled water (TDW), air, dry air (dried using desiccant) and solutions of pH 3, 5, 7, 9, and 11 (the acidity was regulated using nitric acid and sodium hydroxide). The effect of temperature on sample degradation was examined by heating for 30 minutes at temperatures between 40  $^{\circ}\text{C}$  and 140  $^{\circ}\text{C}$  in 10  $^{\circ}\text{C}$  intervals. The coatings were analysed by IRRAS using the same set-up described in Section 2.4, unfortunately due to the use of this technique it was not possible to simulate physiological conditions due to deposition of protein.

## **2.7 Cell Culture**

Human osteosarcoma cells (TE85 HOS, ECACC) were cultured in Dulbecco's modified eagles medium (DMEM, Gibco) supplemented with 10 % v/v foetal calf serum (FCS, Gibco), 2 % v/v HEPES (1 M, Gibco), 1 % v/v glutamine (200 mM, Gibco), 1 % v/v non-essential amino acids (10 mM, Gibco). The cells were trypsinised at 80 % confluency. The samples analysed for initial cell attachment were polished titanium, silanised titanium, silanised titanium reacted with sulfo-SMCC crosslinker, and titanium with fully coupled peptide. Before seeding samples were sterilised with ultra-violet radiation for a minimum of 1 hour on both the top and bottom surfaces. Cells were harvested and seeded on samples at a density of 10000 cells  $\text{cm}^{-2}$  and left for 90 minutes in both serum-free and serum-containing media.

## **2.8 Cell Fixing and Staining**

After attachment, cells were fixed using paraformaldehyde (4 wt % in PBS), permeabilised at 4  $^{\circ}\text{C}$  and then stained using propidium iodide (0.1 % w/v, Sigma) for 1 s. Samples were mounted under glycerol with 10 % diazabicyclo(2,2,2)octane (DABCO, 2  $\text{mg ml}^{-1}$  in PBS)), and 22 areas sampled. Cells were counted using Image Pro Plus software (Media Cybernetics, Maryland) to quantify adhesion. A Philips XL30 scanning electron microscope (SEM) with an accelerating voltage of 15 kV and a working distance of 10 mm was used to examine cell morphology and spreading. Samples for SEM viewing were harvested and seeded in the same manner as

before. Cells were fixed with glutaraldehyde (3 % v/v), post- fixed with 1 % w/v osmium tetroxide solution for 1 h, then left in 7 % sucrose solution in cacodylate buffer (0.1 M) overnight at 4 °C, then dehydrated with; 20, 40, 60, 70, 80 and 90 % v/v ethanol for 5 min, then twice in 100 % ethanol for 10 min, and then dried twice in hexadimethyldisilazane (HMDS) for 5 min, then again for 10 min and finally left to air dry. Samples were gold coated before viewing to prevent charging.

## **2.9 Statistical Analysis**

Error bars depicted are calculated standard errors and significance calculated using one-way ANOVA with Tukey's post-test using Prism software (Graphpad, California). A sample size of three was used for each data point, with each being analysed by the relevant technique at least three times. With the cell tests a sample size of 6 was used; the cell density per sample was found from microscope images of 22 areas of size  $250\ \mu\text{m}^2$ , the cell area was found after measurement of >30 cells per sample using a SEM microscope.

## **3 Results**

### **3.1 Optimisation of Reaction Conditions**

Grazing angle infrared absorbance spectroscopy was used to quantify the coupled reagents at each reaction stage. Selected peaks for each reagent (Si-CH<sub>3</sub> for silane at 1230-1270  $\text{cm}^{-1}$ , amine for cysteine at 1450-1660  $\text{cm}^{-1}$ , or imide for the sulfo-SMCC crosslinker at 1685-1730  $\text{cm}^{-1}$ ) were integrated with a linear baseline.

The use of a nitrogen atmosphere and oxidising the titanium was shown to have a significant effect on the degree of silanisation with the oxidation treatment showing a significant improvement, as seen in figure 2. To examine the degree of silanisation with increasing time, the reaction was modelled empirically using an exponential association and the time chosen for subsequent reactions that corresponded to 90 % of the maximum. The model fit is demonstrated in figure 3a and reached 90 % of the maximum at a time of 194 min.

The optimal concentration of reactants was also decided through modelling with an exponential association and the concentration chosen when 90 % of the maximum was reached. The optimum concentrations were found to be 3.7 % v/v silane, see figure 3b, 1.1  $\text{mg ml}^{-1}$  of sulfo-SMCC, see figure 3c, and 2.1  $\text{mg ml}^{-1}$  of cysteine, see figure 3d.

### **3.2 Topographical Analysis of Silanised Surfaces**

The topographical structures produced with trifunctional and monofunctional silanes can be seen in figure 4. The trifunctional silane produced large clusters of material (1-5  $\mu\text{m}$  spacing) resulting in non-uniform topographies. The monofunctional silane had a lower roughness and presented a more uniform surface. When the monofunctional silanised surface was then functionalised with cysteine an increase in roughness was observed, figures 4 and 5. The topography of the final coupled surface consisted of patches of increased height with an average spacing distance of 5  $\mu\text{m}$ .

### **3.3 Surface elemental compositions**

XPS data was analysed with Casa XPS software (<http://www.casaxps.com>). Deconvolution of the oxygen (O) peak was carried out using a linear background, the full width half maximum of all O 1s peaks were set to equal that of the titanium dioxide peak at 529.2 eV. The remaining three peaks assigned were; carbon bound oxygen, hydroxyl groups, and water with shifts from the titania peak of 2.37, 1.39, and 3.71 eV respectively, the fit is demonstrated in figure 6. All elements were normalised by the titanium peak intensity to account for masking effects.

The surface elemental compositions of the samples are illustrated in table 1. After silanisation a dramatic increase was seen in the nitrogen, carbon, silicon and combined oxygen peaks from hydroxyl groups, water and carbon. After crosslinking, these peaks decreased to a level similar to than that of the untreated titanium. After functionalisation with cysteine no significant increase in the nitrogen and carbon peaks was observed.

### **3.4 Thickness of coupled layers**

The DPI results confirmed successful functionalisation by an increase in thickness of the chip at each stage. An increase of  $0.89 \pm 0.09$  nm was seen when the sulfo-SMCC was flowed through the chip and a smaller increase of  $0.01 \pm 0.09$  nm after the cysteine, see figure 7, though this was not within the experimental error of the instrument. It was not possible to analyse the silane thickness using the DPI due to unwanted reactions with tubing in the machine. Instead the monofunctional silane was modelled using Materials Visualiser (Accelrys<sup>®</sup>), a comparison of the measured thickness values and the modelled thicknesses are illustrated in table 2. The



total thickness values correlate well and show that, presuming the surfaces react uniformly and in a monolayer, a thickness of 1.7 nm would be expected.

### 3.5 *Stability tests*

Degradation of the cysteine coupled surfaces was monitored using infrared spectroscopy over a period of 8 days. Results were fitted empirically with a 1<sup>st</sup> order polynomial line of best fit through  $y = 100\%$ . The amine region was integrated with a linear baseline across the region  $1451\text{--}1662\text{ cm}^{-1}$ . Increased degradation was seen on samples exposed to a greater humidity in the surrounding environment, see figure 8a. It was estimated from the trends that the samples kept in water would be fully removed from the surface by 11 days, those in air by 11 days 6 hours and in the desiccator by 12 days and 2 hours.

The acidity of the environment also had a significant effect on the sample degradation, as can be seen in figure 8b. The coating was most stable at a pH of 3. The predicted time for the coating to be completely removed was found to be 11 days (pH 7), 12 days 2 hours (pH 11) 12 days 3 hours (pH 5), 12 days 15 hours (pH 9) and 17 days 7 hours (pH 3).

Through heat treatments of the functionalised surface it was possible to observe the temperature that chemical groups started to leave the surface. The sample spectra, illustrated in figure 9, was compared to that at room temperature and the data normalised; so the peaks show the disappearance of bands and the band assignments are listed in table 3.

No change was observed in the spectra until  $50\text{ }^{\circ}\text{C}$  when a broad peak developed at  $1050\text{ cm}^{-1}$  which was assigned to siloxane bonds, also at this temperature a broad band at  $3100\text{ cm}^{-1}$  was seen due to hydrogen bonded amines. At  $60\text{ }^{\circ}\text{C}$  amine I and II bands due to the cysteine appeared, and an increase was seen in both the  $\nu(\text{C-H})$  bands and silane peaks. In addition to this, peaks appeared at  $3700\text{ cm}^{-1}$  showing that free hydroxyl groups from the titania surface had dissociated. No significant change was seen after this until  $100\text{ }^{\circ}\text{C}$  when there was a dramatic increase in the siloxane bond intensity which appeared to mask the bands from the cysteine. The imide peaks from the sulfo-SMCC crosslinker were not observed clearly until  $140\text{ }^{\circ}\text{C}$ , apart from a small peak at  $100\text{ }^{\circ}\text{C}$ .

### **3.6 Initial Cell Attachment and Spreading**

To test the effect of the surfaces on cell attachment and spreading, 90 minute cell attachment was performed on the samples at each stage of functionalisation in both serum-free and serum-containing media. The cell attachment was measured using propidium iodide staining then cell counting, and the cell morphology was examined using SEM and the cell areas quantified using Image J software (<http://rsb.info.nih.gov/ij/>). When cultured in serum-containing media the untreated titanium surfaces showed high cell density of cells as can be seen from figure 10a; these were used as the positive control. Significantly lower cell density was noted on the silanised surfaces; however, an improvement in cell response was observed after crosslinking of sulfo-SMCC and cysteine functionalisation resulting in a greater cell density than the titanium control. The cell density on surfaces cultured in serum-free media had the same trends although with fewer cells. The cell area results shown in figure 10b correspond with the cell density results; poor cell spreading was observed on silanised surfaces but after functionalisation the spreading increased to values comparable to the control. The cell morphology on the untreated titanium surfaces showed evidence of filopodia and lamellopodia formation while more rounded cell morphologies were seen on silanised surfaces, and the crosslinked and cysteine coupled surfaces had a flatter morphology with filopodia clearly visible. The attachment in serum-free media had the same trends as serum-containing, though the cells were generally less spread and more rounded.

## **4 Discussion**

When carrying out silanisation using trifunctional silanes it is common to use a dry nitrogen atmosphere to keep siloxane reactions to the surface monolayer, minimising polymerisation reactions between the silane chains away from the surface. The hypothesis behind the oxidation process is that it would generate more surface hydroxyl groups on the titania, these increased hydroxyl groups allow more silane molecules to bind to the surface. However, the nitrogen atmosphere was shown to improve the monofunctional surface reaction, significantly more than the effect of oxidising the titanium surface, see figure 2. It is not possible for the monofunctional silane to form networks on the surface therefore the nitrogen atmosphere must be important to help prevent dimerisation of the silane molecules promoting reactions with the surface.

A wide variety of trifunctional silane reaction times have been used, the longer times have been reported to result in greater polymerisation and less uniform structures [14]. It was demonstrated in figure 3a that to get

optimum reactions using the methods shown here with APDMES a time period of around 3 hours was required.

Topographical examination of the difference between trifunctional and monofunctional silanised surfaces in figure 4 illustrated how networking of the trifunctional silane affects the surface structure creating clusters of organic material, and that the controlled conditions used here did not produce a monolayer. Several groups claim to produce monolayers of silane with APTES, but this is often not supported by sufficient characterisation [15, 16] and this trend has been noted previously in the literature by Olmos et al. [11]. Vandenberg et al [14] carried out a careful study on the optimum reaction conditions of APTES and showed that short reaction times, low concentrations and short curing times are necessary to minimise polymerisation of the silane.

In this work, the optimum conditions were carefully chosen for APDMES and the samples were treated with APTES in the same manner. When surfaces were functionalised with APDMES in a three stage reaction, increased roughness was observed after each stage (see figure 5, therefore showing that the layers were not being deposited uniformly. In contrast, the monofunctional silane layer had a relatively uniform surface with a roughness only twice that of polished titanium, however small defects would have been multiplied when the upper layers were reacted. The final surface had clusters of organic material with distances approximately 5  $\mu\text{m}$  apart, with a roughness of almost 10 times that of polished titanium. If functionalisation were carried out using the trifunctional silane instead of the monofunctional silane, because the initial surface was an order of magnitude rougher it would therefore be expected that these features would roughen further. These results thus illustrate the advantages of using a monofunctional silane for surface functionalisation.

The success of the coupling reactions was confirmed by XPS analysis of the surfaces at each stage, see table 1. Results showed increased intensity in expected peaks from the silane (carbon, nitrogen, silicon and oxygen). These peaks decreased upon crosslinking but not to below that of untreated titanium, this is most likely because silane is being washed from the surface. The silane has already been washed with toluene which will have removed physically adsorbed species, therefore it is inferred that the PBS is causing hydrolysis of the silane from the surface resulting in the further decrease seen.

From the DPI results and modelling, it is estimated that a monolayer of the coupled material would be approximately 1.7 nm thick of which the monofunctional silane component of 0.73 nm. This value assumes that the organic material has formed a uniform monolayer. It is clearly seen from the AFM results in figure 5 that the final surface structure was much greater in thickness than 1.7 nm, as the z-range is 410 nm. Thus a monolayer of coupled biomolecules was not being produced, even though the specificity of the reactions should not result in any networking. It is suggested that this was due to hydrogen bonding (Kowalczyk et al. [17] showed that silanes can be in two states, bound by the ethoxide group, or by the amine) resulting in the build-up of organic material. Despite the build-up, the resultant surface is shown to be a significant improvement compared to trifunctional silanes.

It has been stated by researchers [17, 10, 11, 13] that monofunctional silanes degrade quicker than trifunctional ones, and often trifunctional silanes are chosen as a result of this. This trend is not agreed by all researchers [11] and quantification of the stability of biomolecules coupled using monofunctional silanes may prove them to be more applicable for biomaterials applications than expected. It was on this basis that the stability tests were carried out to determine the degradation time of the coating in different environments and therefore to obtain a handle on the practicality of such coatings.

The effect of humidity was found to increase degradation because the siloxane bonds are prone to hydrolysis [13]. The infrared results shown in figure 8a are consistent with these findings; the results showed that samples left in water degraded within 11 days, 1½ times faster than those in a desiccator. From this it can be inferred that the silane bonds were the controlling factor in the degradation rate; however, if this were solely the case the degradation curves would fit a pseudo first order kinetic reaction model [11] which is clearly not the case. Therefore, although the silane was the dominant factor in the degradation the other reactants were influencing the rate.

A simple dependence of stability on pH was not observed in the reaction due to the complex degradation of the coupling layers. However, samples at the lowest pH of 3 were shown to be the most stable; although even these were estimated to last only ~18 days. A pH lower than 3 was not tested, although it would be expected that acid hydrolysis would be induced in highly acidic solutions causing increased degradation of the coating. The increased hydrolysis of silanes in basic solutions has been reported previously by Olmos et al [11] and they

also concluded that the detrimental effect of pH is strongest as the functionality of the silane increases, so it is predicted that titanium functionalised using a trifunctional silane would not last as long as the monofunctional coatings reported here.

Thermal treatment of the coatings allowed insight into the chemical structure of the functionalised surfaces. At 50 °C vibrational groups due to the silane (siloxane bonds) were observed, and by 100 °C these bands had increased significantly. The loss at lower temperatures may have been due to physisorbed silanes which were not entirely removed from the washing, and at 100 °C the silanes covalently bound to the surface which require more energy to disassociate started to be removed. The appearance of bands at  $3100\text{ cm}^{-1}$ , were assigned to hydrogen bonded amine groups, and these were observed at 50 °C which supports this theory. It is proposed that the physisorbed monofunctional silane molecules were not washed from the surface because they are hydrogen bonded through the amine end of the molecule. It has been well documented that trifunctional silanes form these structures [17, 13] and is likely that monofunctional silanes behave in the same manner. The amine bands from the cysteine and imide peaks from the crosslinker were observed indicative of successful functionalisation; the cysteine appears to degrade around 60 °C while the crosslinker is stable up to 100 °C.

Cell adhesion and spreading studies supplied valuable in vitro information about the initial cell responses to the functionalised surfaces. The varying cell responses could be influenced by both the surface chemistry and the topography. The AFM results showed a certain degree of variation in the surface topography, however the RMS magnitude only varied between 1 nm and 17 nm and when the roughness was examined against the cell area and density no clear correlation was observed. It was therefore concluded that the cells were responding primarily to the surface chemistry.

After silanisation a significant ( $p < 0.001$ ) decrease in cell density was seen compared to the untreated titanium surface in both serum-free and serum-containing media. Cell spreading was also decreased and the SEM micrographs illustrated very rounded cells with little to no processes visible. This poor cell adhesion could be attributed to the hydrophobic nature of silanised surfaces [19] or it may be an indicator that the silane is toxic to cell function [20]. The observed trend was clearest in the serum-free cell area results, and this may support the theory that it was the hydrophobic nature of the silanised surface that induced the cellular response,

rather than toxicity, for the following reasons. If the media contained serum then the serum proteins would deposit in the first few seconds, changing the surface hydrophilicity and reducing the differences seen between the samples, thus the serum-free media would show increased differences. In addition to this, greater variation was seen in the cell area results compared with the cell density values which imply that the interaction of the cell with the surface was due to cell spreading on the surface and not the initial cell attachment. The cell membrane is primarily composed of a lipid bilayer which has a hydrophilic outer layer; this would be more likely to bind to a hydrophilic surface compared with a hydrophobic one, and this may explain the initial responses to the silanised samples.

After crosslinking and functionalisation the cell density increased to significantly more than the control ( $p < 0.05$ ), spreading also improved to comparable values to the control and SEM micrographs show filopodia formation. This supported the evidence from the characterisation that the final stages of functionalisation were successful, and gave an indication that though the silane had detrimental effects these were negated by the peptide coupling.

With respect to orthopaedic applications, this positive cell response to the coupled surface is encouraging, although more long term studies are required to discover if the underlying silane layer produces problems after degradation [20]. In addition, the lifetime of the coating (11 days in aqueous environments which could approximate physiological conditions) would be long enough to induce a cellular response in vivo; however, would not last the implant lifetime. The lifetime of the coating may be improved through an increase in the length of the alkyl chain of the silane which may improve the packing density resulting in a structure akin to a self-assembled monolayer. Another possibility would be to alter the silane structure to increase its hydrophobicity or steric hindrance, restricting attack by water. If the silane stability were increased the biomolecule would remain attached for longer and potentially induce a greater response. In addition, any detrimental effects of the degradation products would be hindered due to the slowed rate of release. The uniformity of the coatings produced and the simplicity of the reaction procedure could provide an ideal method for examining cell responses to biomolecules in vitro, and this could be a viable alternative to using trifunctional silanes.

The feasibility of using monofunctional silanes for the functionalisation of titanium has been characterised, optimised and addressed in terms of coating stability and initial osteoblast attachment. The use of a monofunctional amino-silane to couple peptides to the surface of titania has been thoroughly characterised and its potential use as a replacement for trifunctional silanes investigated. Functionalisation was shown to be successful and the coating formed was thinner and more uniform than similar trifunctional amino-silane structures. The characterisation revealed that a monolayer was not forming on the surface and that the final coupled surface consisted of aggregates with an average spacing of 5  $\mu\text{m}$ .

Furthermore, this study showed that covalent attachment with monofunctional amino-silanes can produce coatings that will last up to 17 days in an acidic environment. HOS cell adhesion responses to the silane layer was poor, however after crosslinking of the peptide cell responses were improved to a level equivalent to that of the control sample illustrating the success of this coupling method and its potential as a procedure for attaching biomolecules to titanium surfaces.

### **Acknowledgements**

The authors would like to thank Smith and Nephew for their funding and support with this work, and the EPSRC for funding. We would also like to thank Mark Gostock from Farfield Scientific Ltd, UK for his training and advice with the DPI work, and Farfield Scientific Ltd. for the loan of the equipment.

### **References**

1. Nanci A, Wuest JD., Peru L, Brunet P, Sharma V, Zalzal S, McKee MD. Chemical modification of titanium surfaces for covalent attachment of biological molecules. *Journal of Biomedical Materials Research*. 1998;40:324-35.
2. Puleo DA. Biochemical surface modification of Co-Cr-Mo. *Biomaterials*. 1996;17:217-22.
3. Mansur HS, Orefice RL, Vasconcelos WL, Lobato ZP, Machado LJC. Biomaterial with chemically engineered surface for protein immobilization. *Journal of Materials Science: Materials in Medicine*. 2005;16:333-40.
4. White LD, Tripp CP. Reaction of (3-aminopropyl)dimethylethoxysilane with Amine Catalysts on Silica Surfaces. *Journal of Colloid and Interface Science*. 2000;232:400-7.

5. Horne JC, Huang Y, Liu G-Y, Blanchard GJ. Correspondence between Layer Morphology and Intralayer Excitation Transport Dynamics in Zirconium-Phosphonate Monolayers. *Journal of the American Chemical Society*. 1999;121:4419-26.
6. Jonsson U, Olofsson G, Malmqvist M, Ronnberg I. Chemical vapour deposition of silanes. *Thin Solid Films*. 1985;124:117-23.
7. Kanan SM, Tze WT, Y, Tripp C, P. Method to Double the surface concentration and control the orientation of adsorbed (3-aminopropyl)dimethylethoxysilane on silica powders and glass slides. *Langmuir*. 2002;18:623-6627.
8. Kallury KMR, Macdonald PM, Thompson M. Effect of surface water and base catalysis on the silanization of silica by aminopropyl)alkoxysilanes studied by X-ray Photoelectron Spectroscopy and <sup>13</sup>C cross-polarization/magic angle spinning nuclear magnetic resonance. *Langmuir*. 1994;10:492-9.
9. Chrisey L, Lee G, O'Ferrall C. Covalent attachment of synthetic DNA to self- assembled monolayer films. *Nucleic Acids Research*. 1996;24:3031-9.
10. Dubruel P, Vanderleyden E, Bergada M, De Paepe I, Chen H, Kuypers S, et al.. Comparative study of silanisation reactions for the biofunctionalisation of Ti-surfaces. *Surface Science*. 2006;600:2562-71.
11. Olmos D, Gonzalez-Benito J, Aznar AJ, Baselga J. Hydrolytic damage study of the silane coupling region in coated silica microfibres: pH and coating type effects. *Journal of Materials Processing Technology*. 2003;143-144:82-6.
12. Halliwell CM, Cass AEG. A Factorial Analysis of Silanization Conditions for the Immobilization of Oligonucleotides on Glass Surfaces. *Analytical Chemistry*. 2001;73:2476-83.
13. Xu Z, Liu Q, Finch JA. Silanation and stability of 3-aminopropyl triethoxy silane on nanosized superparamagnetic particles: I. Direct silanation. *Applied Surface Science*. 1997;120:269-78.
14. Vandenberg ET, Bertilsson L, Liedberg B, Uvdal K, Erlandsson R, Elwing H, et al.. Structure of 3-aminopropyl triethoxy silane on silicon oxide. *Journal of Colloid and Interface Science*. 1991;147:103-18.
15. Wang Y-P, Yuan K, Li Q-L, Wang L-P, Gu S-J, Pei X-W. Preparation and characterization of poly(N-isopropylacrylamide) films on a modified glass surface via surface initiated redox polymerization. *Materials Letters*. 2005;59:1736-40.



16. Advincula M, Fan X, Lemons J, Advincula R. Surface modification of surface sol-gel derived titanium oxide films by self-assembled monolayers (SAMs) and non-specific protein adsorption studies. *Colloids and Surfaces B: Biointerfaces*. 2005;42:29-43.
17. Xiao S-J, Textor M, Spencer ND. Covalent attachment of cell-adhesive, (arg-gly-asp)- containing peptides to titanium surfaces. *Langmuir*. 1998;14:5507-16.
18. Kowalczyk D, Slomkowski S, Chehimi MM, Delamar M. Adsorption of aminopropyltriethoxy silane on quartz: an XPS and contact angle measurements study. *International Journal of Adhesion and Adhesives*. 1996;16:227-32.
19. Altankov G, Groth T. Reorganization of substratum-bound fibronectin on hydrophilic and hydrophobic materials is related to biocompatibility. *Journal of Materials Science: Materials in Medicine*. 1994;5:732-7.
20. Dupraz Av, De Wijn J, Goedemoed J. Biocompatibility screening of silane-treated hydroxyapatite powders, for use as filler in resorbable composites. *Journal of Materials Science, Materials in Medicine*. 1996;7:731-738.
21. Azour H, Derouault J, Lauroua P, Vezon G. Fourier transform infrared spectroscopic characterization of grafting of 3-aminopropyl silanol onto aluminum/alumina substrate. *Spectrochimica Acta Part A: Molecular and Biomolecular Spectroscopy*. 2000;56:1627-35.
22. Seco AM, Goncalves MC, Almeida RM. Densification of hybrid silica-titania sol-gel films studied by ellipsometry and FTIR. *Materials Science and Engineering B*. 2000;76:193-9.
23. Weigel C, Kellner R. FTIR-ATR-spectroscopic investigation of the silanization of germanium surfaces with 3-aminopropyltriethoxysilane. *Analytical and Bioanalytical Chemistry (Historical Archive)*. 1989;335:663-8.
24. Sata EK. Controlled preparation of amino-functionalised surfaces on porous silica by atomic layer deposition. *Inorganic Chemistry Publication Series No 4*. 2004.
25. Baraton M-I, Merhari L. Surface chemistry of TiO<sub>2</sub> nanoparticles: influence on electrical and gas sensing properties. *Journal of the European Ceramic Society*. 2004;24:1399-404.

## Figures and Tables

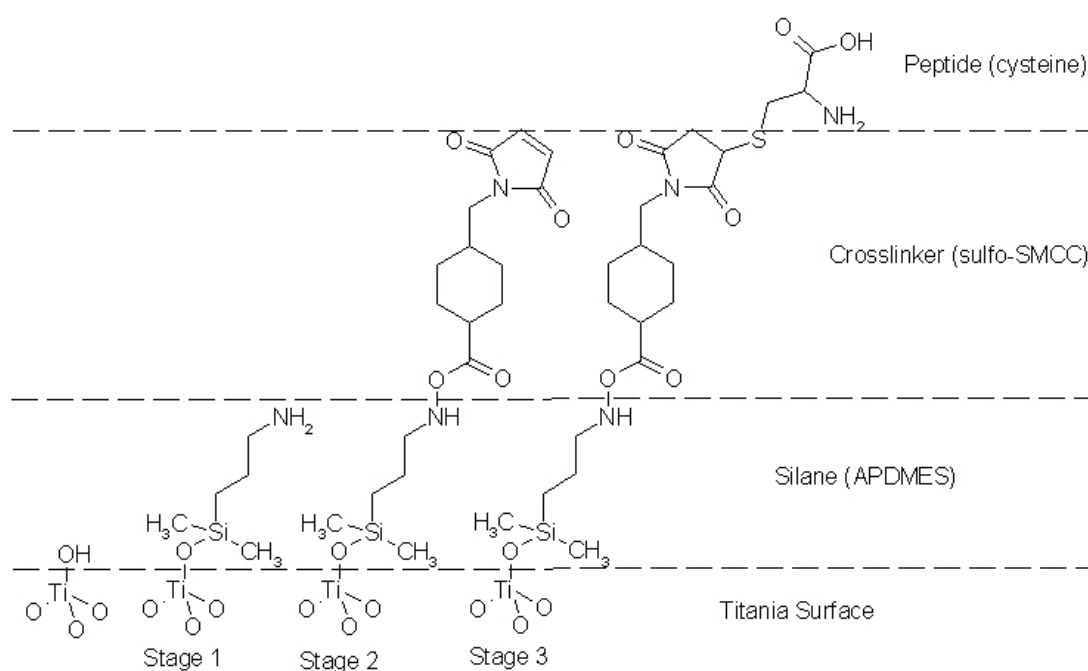


Figure 1. Schematic of the coupling protocol used to functionalise titanium surfaces with peptide in three stages. An aminosilane was reacted at the first stage, a heterobifunctional crosslinker at the second stage, enabling the reaction of the peptide at the final stage.

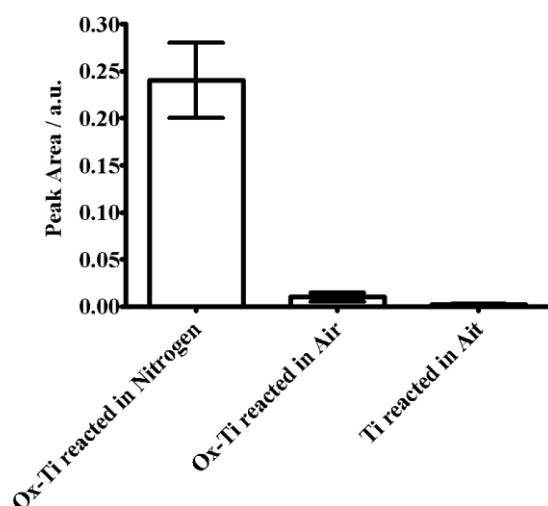


Figure 2. Integration of FTIR absorbance of  $\text{Si-CH}_3$  band from  $1230\text{ cm}^{-1}$  -  $1270\text{ cm}^{-1}$  with a linear baseline. Oxidised titanium samples (Ox-Ti) and untreated titanium samples (Ti) were silanised with 4 % APDMES for 1 h in air and in a dry nitrogen atmosphere. A sample size of three was used for each data point and the error bars represent the standard error in the mean.

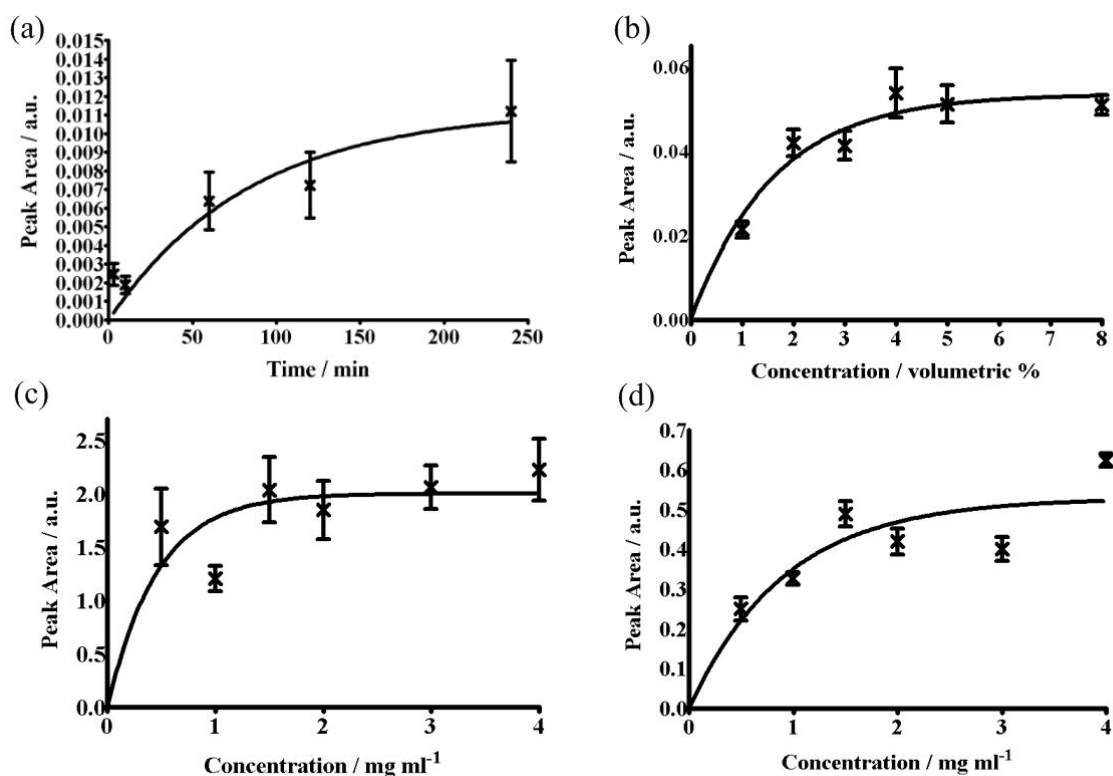


Figure 3. Integration of FTIR absorbance of (a) Si-CH<sub>3</sub> band with increasing silanisation time, using 4 % v/v silane concentration, (b) Si-CH<sub>3</sub> band over a range of silane concentrations, (c) imide band from over a range of sulfo-SMCC concentrations, after reacting with 4 % silane, (d) amine band from over a range of cysteine concentrations, after reacting with 4% silane and 1.5 mg ml<sup>-1</sup> of sulfo-SMCC. A sample size of three was used for each data point and the error bars represent the standard error in the mean.

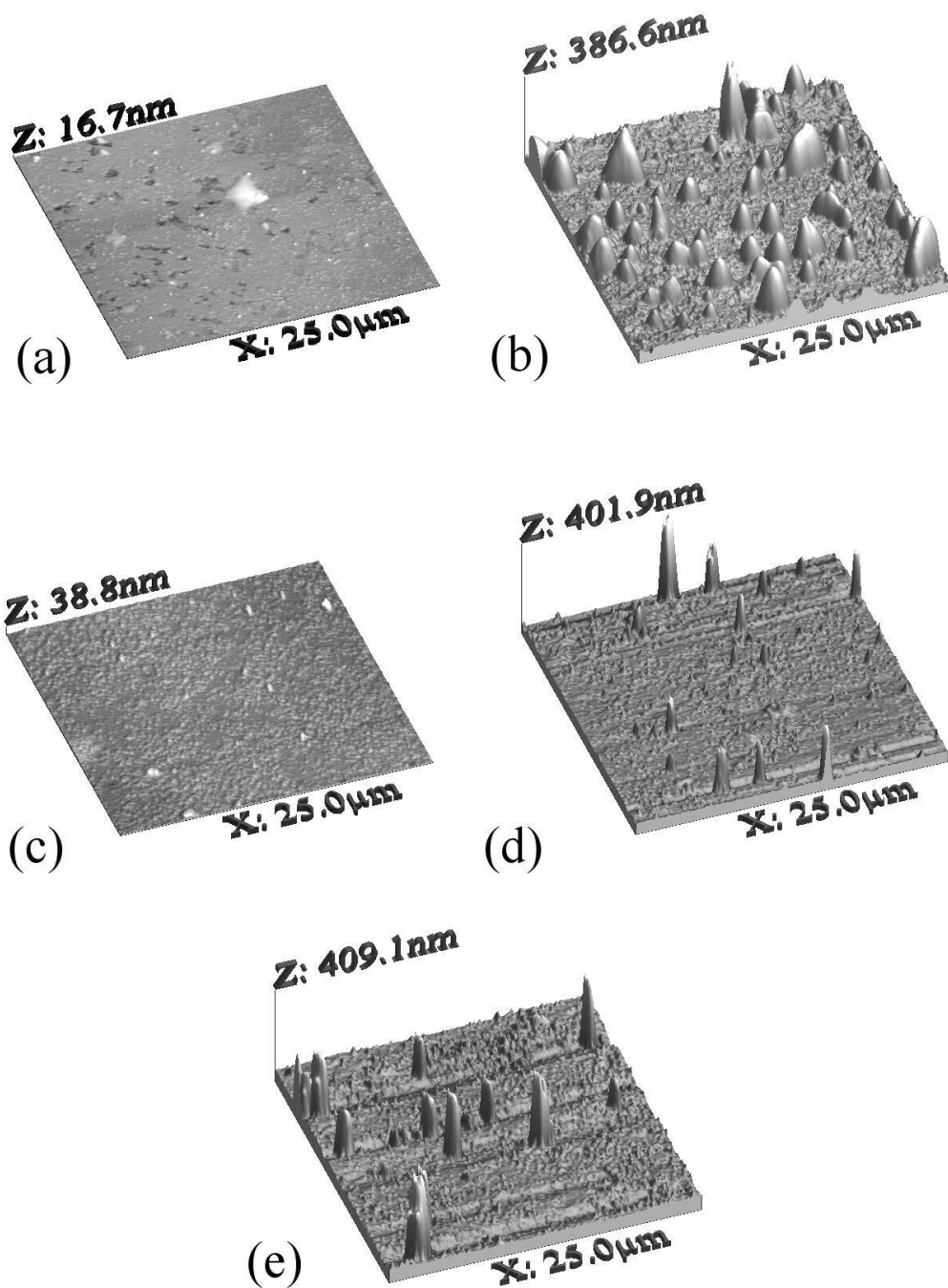


Figure 4. Representative AFM pictures over a  $125.5\text{ }\mu\text{m}^2$  area of samples at different stages of functionalisation compared with a trifunctionally silanised surface; (a) untreated titanium (b) reaction with 4% APTES (c) stage 1. reaction with 4% APDMES (d) stage 2 reaction with  $1.5\text{ mg ml}^{-1}$  sulfo-SMCC (e) stage 3 reaction with  $2\text{ mg ml}^{-1}$  cysteine. A sample size of three was used for each data point and the error bars represent the standard error in the mean.

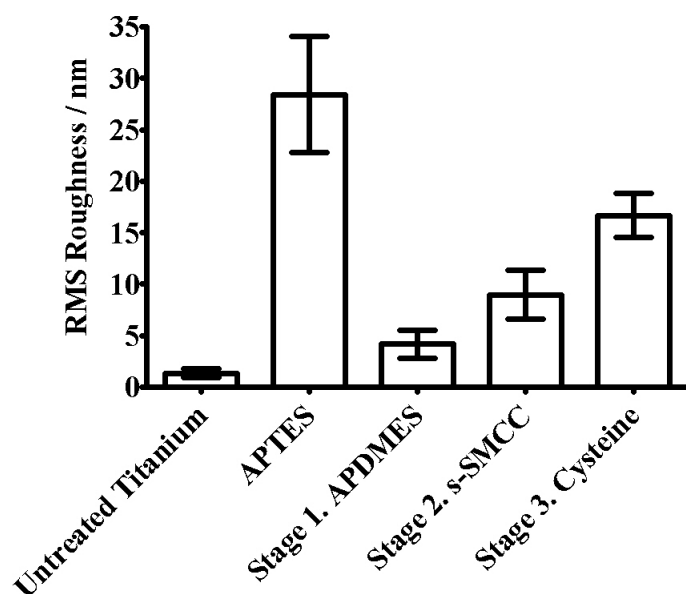


Figure 5. RMS roughness values calculated from AFM micrographs; a sample size of 3 was used and the error bars represent by the standard error in the mean.

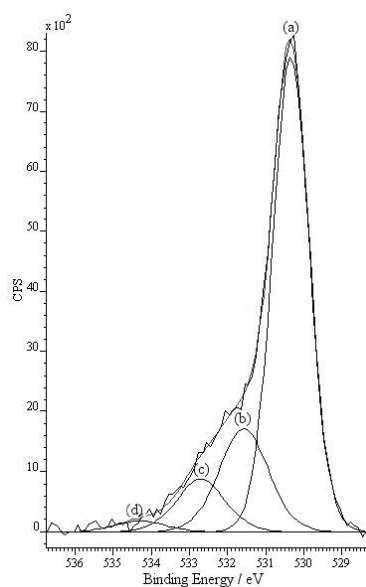


Figure 6. Illustration of deconvolution of the O 1s XPS peak (a) oxygen bound to titanium (b) hydroxyl groups (c) oxygen due to carbon (d) water.

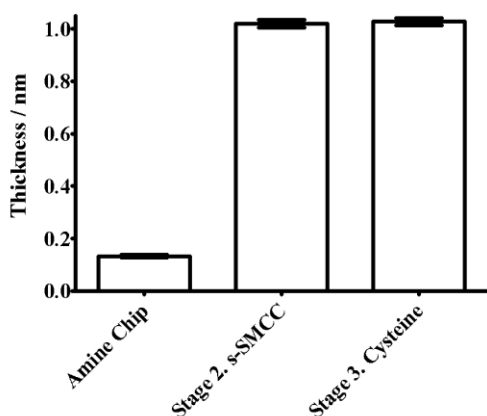


Figure 7. Thickness after reaction of sulfo-SMCC ( $1.5 \text{ mg ml}^{-1}$ ) and cysteine ( $3 \text{ mg ml}^{-1}$ ) with an amine functionalised chip analysed using DPI. A sample size of three was used for each data point and the error bars represent the standard error in the mean.

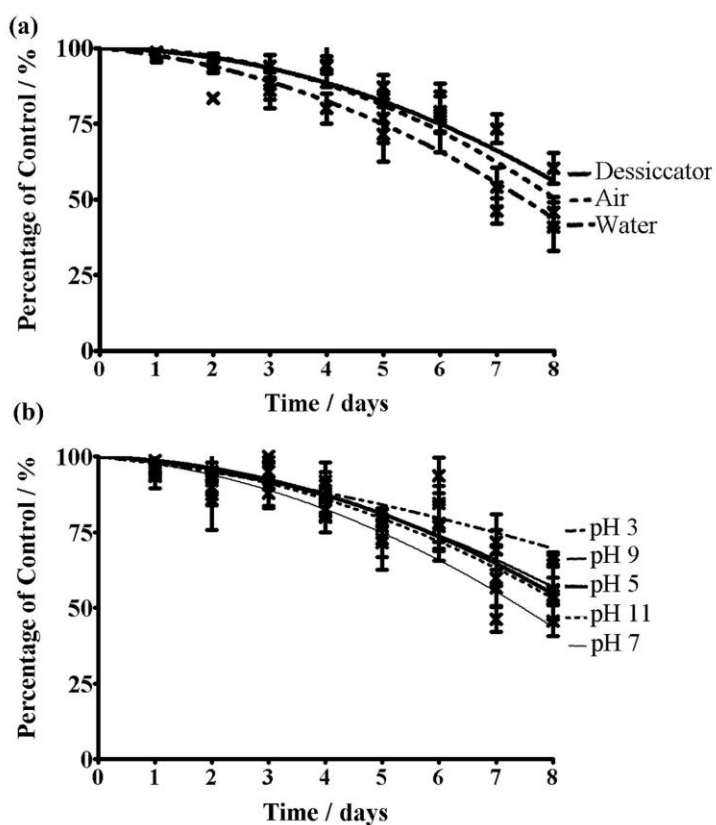


Figure 8. Degradation of cysteine functionalised samples in different (a) humidities and (b) acidities over a period of 8 days. Degradation of coating monitored through the infrared amine band; a sample size of three was used for each data point and the error bars represent the standard error in the mean.

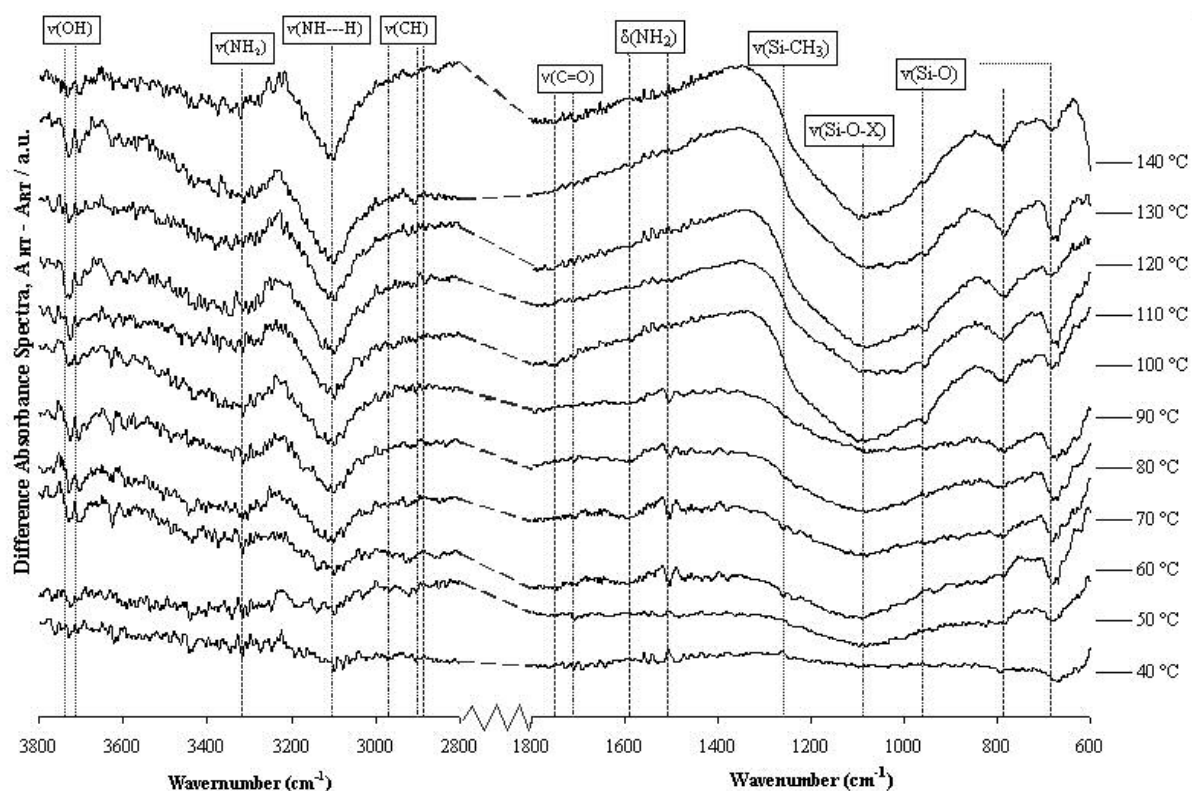


Figure 9. Infrared spectra after incremental heat treatments (AHT) of cysteine functionalised titanium samples up to 140 °C, the difference spectra illustrated and a sample at room temperature was used as a control (ART). Region from 600-3800  $\text{cm}^{-1}$  shown. Each data point represents the average of a sample size of three.

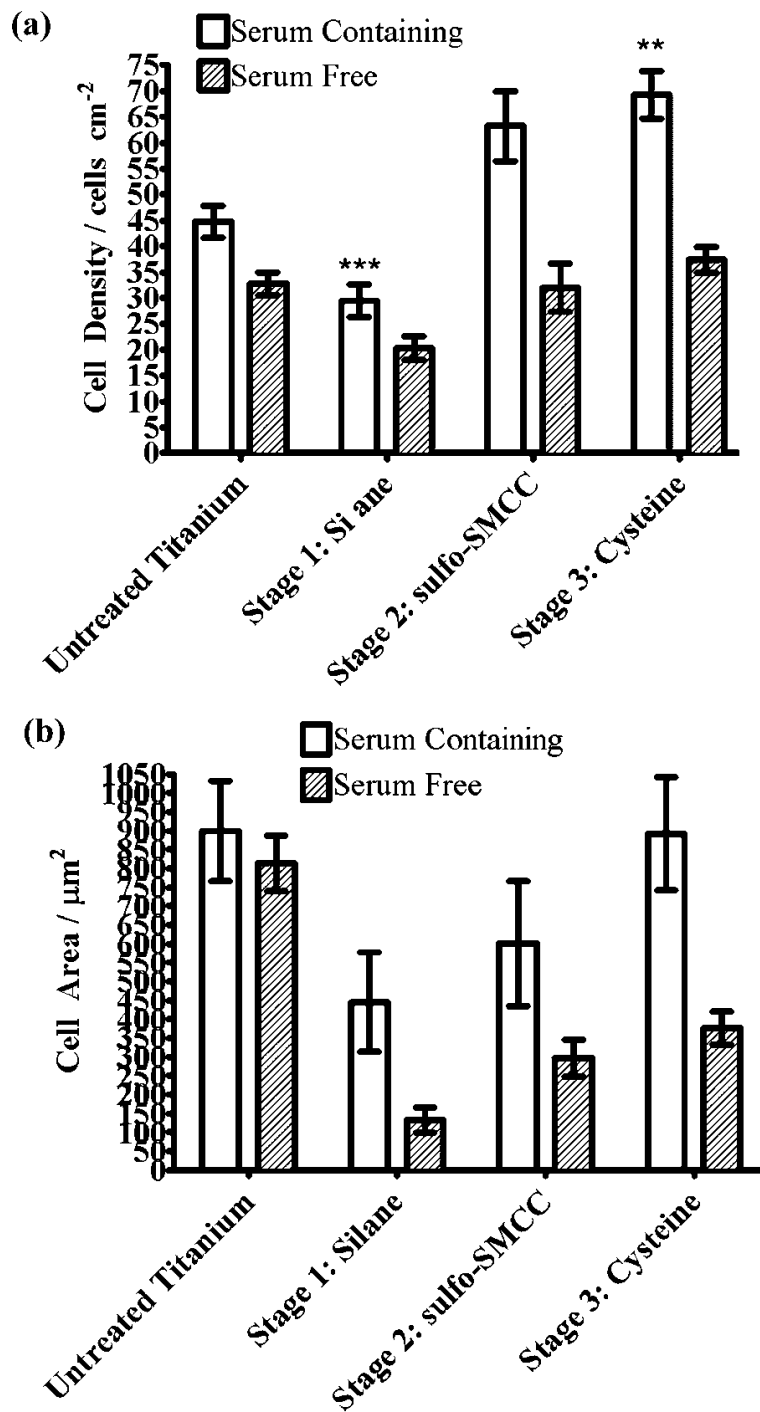


Figure 10. Cell areas (a) and cell density (b) measured on titanium samples at different stages of peptide functionalisation when cultured for 90 minutes in both serum containing and serum free media using fibronectin as a control. Significance compared to the untreated titanium of  $p < 0.001$  is denoted by \*\*\*, and  $p < 0.05$  is denoted by \*\*. Average cell area was calculated from a sample size of three with SEM micrographs measured of  $> 30$  cells per sample, the cell density was found for each sample from 22 microscope images of size  $250 \mu\text{m}^2$ .



	O 1s from TiO	O 1s from H <sub>2</sub> O, OH, C	N 1s	C 1s	Si 2p
Untreated Titanium (Ti)	1.73 ( $\pm 0.04$ )	0.53 ( $\pm 0.05$ )	0.00 ( $\pm 0.01$ )	0.45 ( $\pm 0.04$ )	0.00 ( $\pm 0.01$ )
Monofunctional Silanised Ti	1.66 ( $\pm 0.04$ )	1.00 ( $\pm 0.37$ )	0.15 ( $\pm 0.07$ )	0.85 ( $\pm 0.34$ )	0.23 ( $\pm 0.12$ )
Crosslinked Silanised Ti	1.68 ( $\pm 0.03$ )	0.66 ( $\pm 0.09$ )	0.05 ( $\pm 0.01$ )	0.45 ( $\pm 0.06$ )	0.04 ( $\pm 0.01$ )
Cysteine functionalised Ti	1.78 ( $\pm 0.03$ )	0.63 ( $\pm 0.07$ )	0.07 ( $\pm 0.02$ )	0.49 ( $\pm 0.09$ )	0.04 ( $\pm 0.01$ )

Table 1. XPS results showing variation in elemental percentage (normalised by titanium peak area) on different chemically coupled surfaces. The data points were acquired from a sample size of three and the error represents the standard error in the mean.

	Measured Thickness (nm)	Modelled Thickness (nm)
Stage 1. Monofunctional Silane	-	0.75
Stage 2. Sulfo-SMCC	0.89 ( $\pm 0.09$ )	0.89
Stage 3. Cysteine	0.01 ( $\pm 0.09$ )	0.06
TOTAL	1.65 ( $\pm 0.18$ )	1.70

Table 2: Comparison of measured and predicted coating thicknesses. (Note. The total measured thickness value includes the modelled value for the silane thickness, due to lack of data). A sample size of three was used for each data point and the error bars represent the standard error in the mean.

Wavenumber (cm <sup>-1</sup> )	Assignments	Description	Reference
670	v(Si-O)	Siloxane bonds	[21]
800	v(Si-O)	Siloxane bonds	[21]
955	v(Si-O-Ti)	Siloxane bonds	[22]
1078	v(Si-O-X)	Siloxane bonds	[4, 23]
1253	v(Si-CH <sub>3</sub> )	Methyl	[22]
1503	$\delta$ (NH <sub>2</sub> )	Amine I	[4, 7, 24]
1592	$\delta$ (NH <sub>2</sub> )	Amine II	[4, 7, 24]
1720	v(C=O)	Carboxyl from imide ring	[14]
1775	v(C=O)	Carboxyl from imide ring	[14]
2800-3000	v(CH)	Alkyl groups	[3, 21]
3100	v(NH <sub>2</sub> ---H)	Hydrogen bonded amine	[21]
3320	v(NH <sub>2</sub> )	Free amine	[4, 21, 24]
3700	v(OH)	Free hydroxyl	[25]
3730	v(OH)	Free hydroxyl	[25]

Table 3. Assigned peak positions of chemical groups. v = stretching vibrations and C = bending vibrations, the X denotes either a silicon or carbon atom.